Calibration of Millimeter-Wave Polarimeters Using a Thin Dielectric Sheet

Christopher W. O'Dell, Daniel S. Swetz, and Peter T. Timbie

Abstract—We present the theory and application of a novel calibration system for millimeter and microwave polarimeters. The technique is a simple extension of the conventional wire-grid approach, but employs a thin dielectric sheet rather than a grid. The primary advantage of this approach is to obtain a calibration signal that is only slightly polarized, which can be beneficial for certain applications such as astronomical radiometers that measure very low levels of polarization, or systems with a small dynamic range. We compare this approach with other calibration techniques and discuss its successful use in the calibration of the polarization observations of large angular regions experiment, designed to measure polarization in cosmic microwave background radiation.

Index Terms—Calibration, microwave receivers, polarization, radiometry.

I. INTRODUCTION

CALIBRATION is a critical step in the design and use of millimeter-wave radiometers and many different techniques have been developed. In order to calibrate polarimeters, a classic wire-grid approach has traditionally been used [1], [2], the properties of which have been explored by several authors (e.g., [3]–[6]). However, this technique has the disadvantage of generating a large fully polarized calibration signal, as well as being difficult to build for certain applications. Another approach is to use reflection of a known (unpolarized) source from a metal surface [7]; the metal surface induces a small well-characterized polarization [8]. For astrophysical measurements, it is sometimes feasible to calibrate using a celestial object that emits a known polarized signal [9].

However, sometimes none of these techniques are suitable for a given polarimeter, especially in the case of polarimeters with a small dynamic range. This was the case for the polarization observations of large angular regions (POLAR) instrument [10], with which we searched for polarization in the cosmic microwave background radiation. POLAR is a correlation polarimeter [9], which employs double-balanced mixers to correlate the two orthogonal polarizations selected by an orthomode transducer in order to directly measure the polarization of the incoming signal. However, these mixers had a very narrow range of linearity (approximately 6 dB in power) and the calibration signal from a wire grid was well outside this range. Calibration
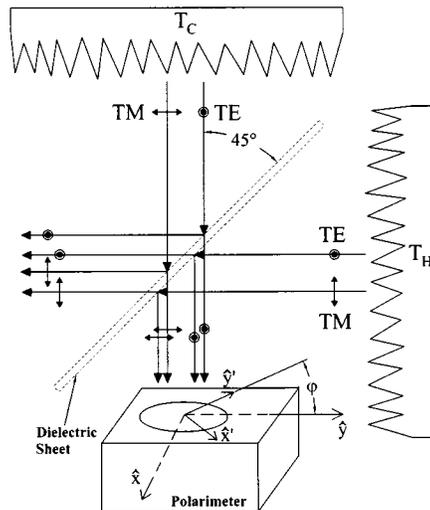
Fig. 1. Calibration setup using the thin dielectric sheet. Unpolarized radiation from both a hot load (side) and cold load (top) is partially polarized due to the slight difference in R_{TE} and R_{TM} of the sheet, thus causing the polarimeter to see a slightly polarized signal. The angle between the polarimeter x-axis and sheet plane of incidence is ϕ. The Stokes parameters can be modulated by variation of the angle ϕ.

with a nutating metal flat would have overcome this limitation, as it is capable of providing the necessary small polarization signal, but was infeasible given our equipment's geometric constraints. Thus, we explored a slightly different avenue for calibration of the instrument, i.e., reflection of thermal radiation off a thin dielectric sheet.

II. CALIBRATION TECHNIQUE

In order to calibrate POLAR, we replaced the wire grid in the conventional setup with a thin dielectric sheet whose composition and thickness were chosen as described below (see Fig. 1). If the reflection and emission properties of the sheet can be ascertained, through either direct measurement or calculation, then it is straightforward to calculate the expected signal from the dielectric. Both the hot and cold loads emit blackbody radiation at their physical temperatures T_H and T_C, respectively. These unpolarized sources emit an equal amount of radiation polarized both perpendicular (TE) and parallel (TM) to the plane of incidence of the dielectric sheet. Note that the TE and TM radiation fields are *uncorrelated* with each other. Upon traversal of the sheet, a certain amount of each of these four fields arrive at the aperture of the polarimeter, along with the oblique emission from the sheet itself (which has a physical temperature T_S).

In order to perform the calibration, we must determine the intensity of fields at the aperture of the polarimeter from the cal-

ibrator. We use the standard Stokes parameters $\{I, Q, U, V\}$ to characterize field intensity. The Stokes parameters are additive quantities and, hence, simplify the following mathematics.

In [2], the Stokes parameters from a wire-grid calibrator are calculated. For the dielectric sheet, the derivation is similar, but we must also take into account the emissivity of the sheet, which may not be negligible. We will make the simplifying assumption that the microwave absorbers (T_C and T_H) are perfect blackbodies; this assumption will be discussed later in detail.

First let us calculate the Stokes parameters in the reference frame of the calibrator; once we have these, it is straightforward to "rotate" them into the frame of the polarimeter. We give the Stokes parameters in units of brightness temperature. For a single-mode antenna in the Rayleigh-Jeans limit, the brightness temperature T_B is related to power P through $P = \Delta\nu k_B T_B$, where $\Delta\nu$ is the frequency bandwidth and k_B is Boltzmann's constant. Let $\hat{x}$-$\hat{y}$ be the coordinate system of the calibrator and $\hat{x}'$-$\hat{y}'$ be the coordinate system of the polarimeter; ϕ denotes the rotation angle between these reference frames. Further, let I_x and I_y correspond to the brightness temperature of the total power polarized along $\hat{x}$ and $\hat{y}$, respectively.[1] The Q Stokes parameter is given by $Q = I_x - I_y$. The brightness temperatures I_x, I_y, Q, and U in the (unprimed) calibrator coordinate system will be (see Appendix I)

$$I_x = T_C + (T_H - T_C) R_{\text{TE}} + (T_S - T_C) \epsilon_{\text{TE}} \tag{1a}$$

$$I_y = T_C + (T_H - T_C) R_{\text{TM}} + (T_S - T_C) \epsilon_{\text{TM}} \tag{1b}$$

$$Q = (T_H - T_C)(R_{\text{TE}} - R_{\text{TM}}) + (T_S - T_C)(\epsilon_{\text{TE}} - \epsilon_{\text{TM}}) \tag{1c}$$

$$U = 0. \tag{1d}$$

If the angle between the polarimeter $\hat{x}'$-axis and the sheet plane of incidence ($\hat{x}$-axis) is ϕ, then the Stokes parameters as seen by the polarimeter are given by

$$I_{x'} = I_x \cos^2 \phi + I_y \sin^2 \phi \tag{2a}$$

$$I_{y'} = I_x \sin^2 \phi + I_y \cos^2 \phi \tag{2b}$$

$$Q' = Q \cos 2\phi \tag{2c}$$

$$U' = -Q \sin 2\phi. \tag{2d}$$

We note here that including the small reflectance R_l of the unpolarized loads would have the effect of increasing T_C to $T_C + R_l(T_H - T_C)$ in the reflection term in (1), assuming the environment has a temperature T_H. Typically the loads can be chosen such that the overall effect can be neglected. If this is not possible, R_l must be measured at the frequencies of interest, so that its effect on (1) can be included.

It is then a simple matter to calibrate the polarimeter by varying the angle ϕ, either by rotating the calibrator or polarimeter. As we are primarily interested in calibrating polarization channels, we will focus on the Q- and U-calibration signals; each of these changes by a full 100% over a complete ϕ cycle. In contrast, varying ϕ produced very low signal-to-noise variations in $I_{x'}$ and $I_{y'}$ for the dielectric sheets we used,

making a "total power" calibration with the sheet impractical. However, this is inconsequential because those channels are easily calibrated with simple unpolarized loads through a conventional y-factor measurement.

The accuracy of the Q or U calibration depends on several factors. First, one must know or determine the relevant material properties of the sheet, namely, the reflection coefficient and emissivity both for the two polarization states and as a function of incidence angle. The angle of incidence θ must be known to reasonable accuracy. The sidelobes of the receiving horn should be low, the sheet and loads should be large enough to completely fill the main beam of the receiver, and the loads should be near-perfect absorbers or else stray radiation from the surroundings will enter the system. All these conditions must be satisfied in the wire-grid approach as well, with the exception that instead of understanding the grid properties, it is now the reflection and emission properties of the dielectric sheet that we seek to understand. It is on these issues that we will now focus.

III. DIELECTRIC REFLECTION AND EMISSION PROPERTIES

The general situation we wish to consider is as follows. An electromagnetic wave of wavelength λ is incident upon an infinite dielectric sheet of thickness d and index of refraction n. Part of this wave will be reflected, part will be transmitted, and part will be absorbed. All these quantities will depend upon the polarization state of the incident wave, which, in general, will be a combination of TE- and TM-polarized radiation. Thus, for the radiation incident upon the sheet (to be distinguished from its own thermal emission), we have

$$|r|^2 + |t|^2 + A = 1 \tag{3}$$

where $|r|^2$, $|t|^2$, and A represent the fractional power reflected, transmitted, and absorbed, respectively; r and t are the usual Fresnel reflection and transmission coefficients and are complex quantities.

If the sheet is in thermal equilibrium, emission will equal absorption (i.e., $\epsilon = A$). In general, a material has a complex index of refraction $N = n - j\kappa$, where n corresponds to the real index of refraction and κ is the extinction coefficient and determines the loss of the material. If $\kappa \ll n$, then the *loss tangent* of the material, the ratio of the imaginary component to the real component of the dielectric constant, is given approximately by[2]

$$\tan \delta \approx \frac{2\kappa}{n}. \tag{4}$$

Given N, it is possible to calculate both r and t for a lossy dielectric slab [11]. The emissivity ϵ will then be $1 - |r|^2 - |t|^2$ and, in general, will be polarized. However, for this treatment, we assume that the *total* loss in the dielectric is negligible. Section III-C deals with the conditions under which this assumption is valid.

A. Reflection Term—Theory

It is straightforward to derive the reflection coefficients for our smooth dielectric sheet using the Fresnel equations under

---

[1] We work here with the more convenient I_x and I_y rather than their sum I because it is these quantities that polarimeters, such as POLAR, usually measure. Some polarimeters also directly measure Q, U, and/or V, typically via correlation or pseudocorrelation techniques.

[2] The loss tangent $\tan \delta$ is not to be confused with the unrelated quantity δ, the phase change due to the dielectric given in (7).

the assumptions that the dielectric is homogeneous, optically isotropic, nonamplifying, and the wavelength is on the order of or larger than the film thickness, such that all the multiply reflected beams combine coherently (see, e.g., [12] and [13]). Assuming the sheet is placed in air with a refractive index of ~ 1 and absorption by the sheet is neglected, the reflection coefficient can be shown to be

$$R_i = \frac{\left[\cos^2\theta - \gamma_i^2\right]^2 \sin^2\delta}{4\gamma_i^2\cos^2\theta\cos^2\delta + \left[\cos^2\theta + \gamma_i^2\right]^2\sin^2\delta} \quad (5)$$

where $i \in \{TE, TM\}$ represents the incident field polarization direction and

$$\gamma_{\mathrm{TE}} \equiv \sqrt{n^2 - \sin^2\theta} \quad (6a)$$

$$\gamma_{\mathrm{TM}} \equiv \frac{1}{n^2}\sqrt{n^2 - \sin^2\theta} \quad (6b)$$

and where

$$\delta = kd\sqrt{n^2 - \sin^2\theta} \quad (7)$$

is the phase change that the wave undergoes upon traversal of the sheet; $k = (2\pi)/\lambda$ is the wavenumber of the wave in free space, d is the thickness of the sheet, n is the (real) refractive index of the dielectric, and θ is the angle of incidence of the wave upon the sheet.

For this technique, we are primarily interested in the Q and U calibration. From (1c), we see that the quantity of interest here is $R_{\mathrm{TE}} - R_{\mathrm{TM}}$, the difference in the reflection coefficients of the sheet. The coefficients are only the same at normal and grazing incidence; at all other angles, a polarization signal will be produced. The following useful formula can be derived for the case of $\lambda \gg d$ and $\theta = 45°$, conditions which were satisfied by POLAR (see Appendix II):

$$R_{\mathrm{TE}} - R_{\mathrm{TM}} \simeq \left(\frac{\pi f d}{c}\right)^2 \frac{\left(n^4-1\right)\left(n^2-1\right)\left(3n^2-1\right)}{2n^4}. \quad (8)$$

This formula is informative as it shows how the calibration signal behaves with varying frequency, sheet thickness, and index of refraction. Notice the signal varies quadratically in both f and d and even faster with an index of refraction. This implies that all these variables must be known with considerable precision to result in an accurate calibration.

B. Reflection Term—Experimental Verification

We devised a simple system to test the reflection equations presented above in order to verify they worked on real-world materials and to ensure that we had not neglected other potentially important effects. We tested 0.003- (0.076 mm) and 0.020-in-thick (0.51 mm) polypropylene since this material has a well-characterized refractive index of 1.488–1.502 in the useful range of 30–890 GHz [14]. We also tested 0.030–in-thick Teflon. Other materials, such as polyethylene, TPX, or Mylar could of course also be useful and our results are directly applicable to those materials assuming one knows the pertinent material properties.

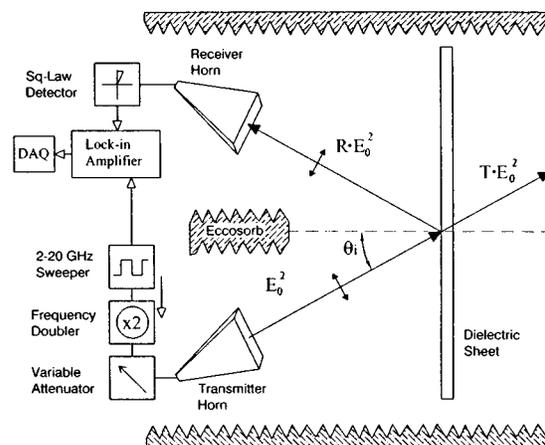The experiments were performed in a small homemade anechoic chamber (see Fig. 2) made of commercially available Ec-

Fig. 2. Experimental configuration used to test the reflectance of various materials. The incidence angle θ_i was kept fixed at $45°$. The frequencies used were the microwave K_a-band (26–36 GHz). The input signal was chopped at 1 kHz to help eliminate $1/f$ noise. The horns are shown here in the TM configuration; for the TE configuration, the horns were rotated $90°$.

cosorb CV-3.[3] Eccosorb CV-3 has a quoted reflectivity of less than -50 dB at frequencies up to 25 GHz and a reflectivity of -34 dB at 107 GHz [15], which was adequate for our purposes. We fixed the incidence angle at $45°$, which was the primary angle of interest to us.[4] A standard-gain (25 dB) pyramidal feedhorn transmitted a signal of known frequency to a dielectric sheet approximately 20 in $\times$20 in in area. The signal was generated by a commercial 2–20-GHz microwave sweeper coupled to a frequency doubler to obtain the K_a-band frequencies of 26–36 GHz. An identical horn was placed symmetrically about the sheet's normal in order to receive the reflected waves. Reflected radiation from the room was found to be minimal. A thin piece of Eccosorb was placed between the two horns to minimize direct coupling between them. The transmitting source was swept through the K_a-band over a period of 100 s and the amplitude square-wave chopped at 1 kHz (this frequency was well above the $1/f$ knee of the system). The received signal was then sent to a lock-in amplifier and recorded by a computer using a simple data acquisition system. The reflected signal was quite small and the lock-in technique enabled us to significantly reduce our sensitivity to $1/f$ noise in the system. A baseline reading was obtained using an aluminum flat instead of the dielectric sheet; the flat had near-perfect reflectivity and provided our normalization.

It was important to control systematic effects well; in particular, the imperfect absorption of microwaves by the Eccosorb walls of the anechoic chamber. By varying the Eccosorb configuration, we were able to virtually eliminate all spurious signals related to imperfect Eccosorb absorption. In the optimal configuration, tests with no reflector showed our system was capable of measuring reflection coefficients as low as a few $\times 10^{-5}$. The primary systematic effect was standing waves in the system propagating between the source and reflecting surface. These were controlled (but not eliminated) by placing an attenuator between the sweeper and transmitting horn.

---

[3]Emerson & Cuming Inc., Canton, MA.

[4]Other angles could potentially be used, but the calculations for the calibration signal would be more complicated than those presented above.
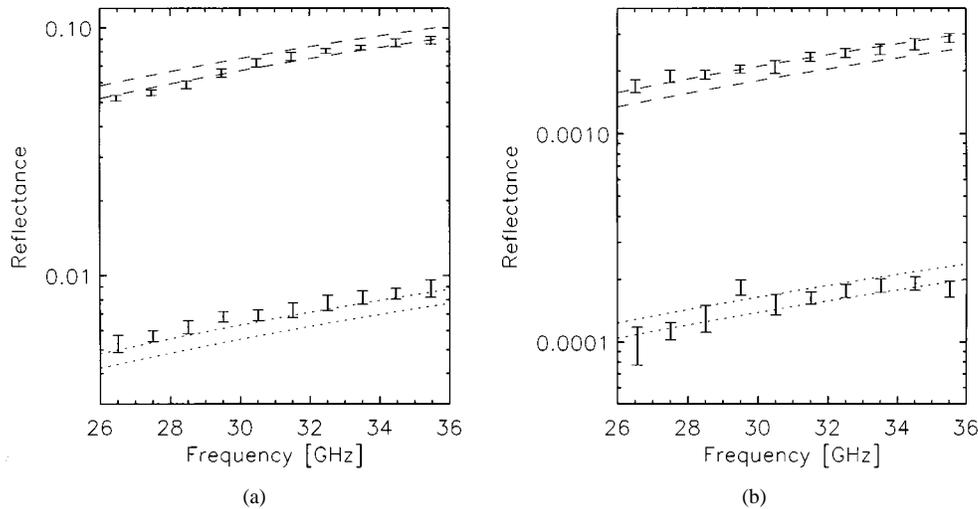
Fig. 3. Comparison between laboratory reflectivity measurements and theory on polypropylene. The displayed 1σ errors in the data are mostly systematic, arising from standing waves in the system. The uncertainty in theory is due to both thickness variations and uncertainties in the index of refraction. R_{TE} corresponds to the upper set of curves (dashed) and R_{TM} to the lower set of curves (dotted). Measurements were averaged into 1 GHz bins for convenience. (a) Results for 0.020-in-thick (0.51 mm) polypropylene. (b) Results for 0.003-in-thick (0.076 mm) polypropylene.

Fig. 3(a) and (b) shows the results for the 0.020- and 0.003-in sheets, respectively. The errors bars shown on the measured points are primarily due to standing waves in the system. The theoretical error contours drawn represent the thickness variations in our plastic sheets. We found that both of these commercial sheets had thickness variations on the order of 5%. Since the reflection signal is roughly proportional to d^2, the resulting uncertainty in the calibration is $\sim 10\%$. Uncertainty in the index of refraction of the dielectric is even more important. Luckily, for our chosen material of polypropylene in the K_a frequency band, the refractive index is known to an accuracy of at worst $\sim 2 \cdot 10^{-3}$ [16], [17], which contributes negligibly to our errors. As Fig. 3 shows, the measured curves match the theory quite well for the displayed polypropylene data. Teflon (not shown) worked equally well, having an $R_{\text{TE}} - R_{\text{TM}}$ of approximately 0.10 for the K_a-band frequencies we tested.

In this section we sought to verify (5) with laboratory experiments. The reader should note that we did not include any off-axis beam effects when calculating the theoretical predictions for these experiments. The general calculation would involve integrating over the antenna pattern of the transmitting and receiving horns, for each polarization state. Off-axis rays, reflecting from the dielectric at slightly different angles from the on-axis rays, will then slightly affect the measured reflection coefficients, due to the variation of the reflection coefficients of the dielectric as a function of angle. However, the remarkable agreement between the predicted (on-axis) and measured reflection coefficients indicates that this was a small effect.

C. The Emission Term

Oblique emission from a dielectric will, in general, be polarized (for a review, see, e.g., [18]). For this calibration technique to work, either the emission must be known accurately (in both polarizations), or it must be negligible. The emission of a material is determined by both its thickness and loss tangent (or alternatively, its extinction coefficient), and will vary as a function of viewing angle and will generally be polarized (i.e., $\epsilon_{\text{TE}} \neq \epsilon_{\text{TM}}$).

As discussed in Section III, the complete way to determine emission involves calculating both R and T using the complex refractive index and then using (3) to find the absorption (which equals the emission in thermodynamic equilibrium); the calibration signal can then be calculated using (1). For this approach to work, the complex index of refraction (and, hence, the loss tangent) must be known to reasonably good accuracy and the surface must be *smooth*; if the surface roughness is too high, the emission polarization will be less than theory predicts [19]. Typically, the loss tangent is known only poorly. Luckily, the *total* emission can often be made small compared to the reflection/transmission terms by the appropriate choice of dielectric material and thickness for the frequencies of interest; one can then simply ignore the emission terms in (1).

An approximation for the total emission is [14]

$$\epsilon \approx \frac{2\pi n \tan \delta}{\lambda} \cdot d \qquad (9)$$

where d denotes the thickness of the emitter and ϵ denotes the fraction of its thermodynamic temperature that is emitted; hence, it produces a brightness temperature of $T_\epsilon = \epsilon \cdot T_S$. As an example, the POLAR calibration used a 0.003-in-thick polypropylene sheet, which had a loss tangent of $\sim 5 \times 10^{-4}$, leading to ~ 12 mK of total emission; this turned out to be small in comparison with the calibration signal and, hence, was neglected.

Fig. 4 shows the ratio of the polarized reflection signal T_{pol} to the emission signal T_e as a function of d/λ. The higher this ratio, the more safely emission can be neglected in calculating the calibration Stokes parameters. Notice that, at higher frequencies and material thicknesses, emission matters *less* than at lower frequencies and thicknesses. This means that the smaller the desired polarization signal, the *more* emission will matter. This result may seem counter-intuitive, but it is directly evident from the reflection and emission equations; emission goes like d/λ, while typically the reflection portion of the signal goes like
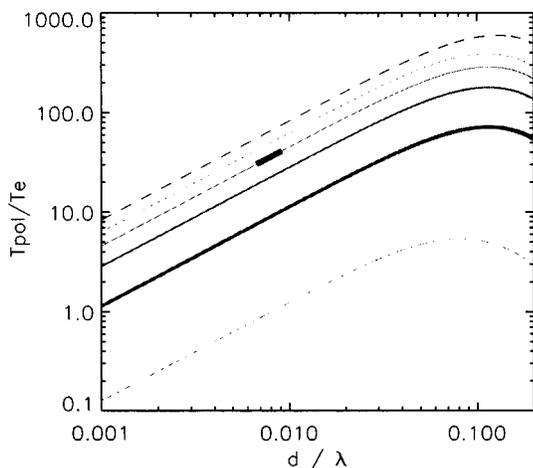
Fig. 4. Ratio of the polarized radiation T_{pol}, due entirely to reflection, to the brightness temperature in emission T_e of the dielectric sheet for various materials versus d/λ, the ratio of sheet thickness to free-space wavelength. The six curves are for different materials and/or frequency ranges. Dashed line: Teflon (30–300 GHz). Dotted line: TPX (30–270 GHz). Solid thin line: polypropylene (20–40 GHz). Solid medium line: polypropylene (40–270 GHz). Solid thick line: polypropylene (270–900 GHz). Dotted–dashed line: Mylar (120–1000 GHz). The darkened box shows POLAR's region in this parameter space. Loss tangents were adopted from [14].

$[d/\lambda]^2$. In terms of absolute emission, polypropylene, polyethylene, TPX, and Teflon are all useful. However, Mylar's high loss makes it nonideal for this technique, unless one has good data on the directional emissivity of the material at the frequencies of interest.

IV. DISCUSSION

The calibration technique presented herein was used successfully to calibrate the POLAR K_a-band receiver in Spring 2000, which recently obtained the best upper limits to date on large angular-scale polarization in the cosmic microwave background [20]. With a 0.003-in polypropylene sheet and using the sky as the cold load (which necessitated measuring the sky temperature independently), we obtained polarized calibration signals of approximately 250, 350, and 500 mK in our three frequency bands of 26–29, 29–32, and 32–36 GHz, respectively. This should be compared to the ~ 250 K signal that we would have obtained from a conventional wire-grid approach; that level of signal was well outside our polarimeter's range of linearity and, thus, was infeasible. The dielectric sheet had the additional benefit of being very simple and inexpensive. Wire grids take time and energy to construct well and can be quite expensive, whereas simple plastic sheets are often easily and cheaply obtained.

However, we discovered several pitfalls in this process that should be avoided if possible. The first is to make sure the dielectric sheet is kept as taut and flat as possible. In our first version of the calibrator, we did not pay much attention to this and the plastic sheet had a slight bow in it. Laboratory results found this bowing to have a significant impact on the resulting calibration signal, causing it to deviate from theory by as much as 20% for a barely visible bowing. Reducing the bowing by increasing the tension in the sheet resulted in the signal matching theoretical predictions.

A second source of error was variation in material thickness. We found that, in practice, some of the materials we tested varied by as much as 10% in thickness across a sheet; this is rather large and leads to a high uncertainty in the calibration signal, due to its approximate d^2 dependence. Sheets with manufacturing processes that lead to a more uniform thickness should be used if possible.

Addressing these basic systematic effects is relatively easy and the result is a simple, inexpensive, and highly tunable calibration system, which can be used in a variety of polarimetric radiometers.

APPENDIX I
DERIVATION OF CALIBRATION SIGNAL STOKES PARAMETERS

Our goal here is to determine the Stokes parameters due to the electric fields generated by the calibrator, as shown in Fig. 1. Let us briefly review the physical basis of the Stokes parameters. The total electric field incident upon our polarimeter can be written as

$$\vec{E} = E_x \hat{x} + E_y \hat{y} \tag{10}$$

where

$$
\begin{aligned}
E_x &= E_{x_0} e^{j(kz - \omega t + \phi_x)} \\
E_y &= E_{y_0} e^{j(kz - \omega t + \phi_y)}.
\end{aligned}
$$

In these equations, the conventional notations of t for time and ω for angular frequency are used. It is implicit that one takes the real part of $\vec{E}$ to obtain the physical field. We define the Stokes parameters for monochromatic radiation in the usual way (see, e.g., [9]) as

$$I = \langle E_{x_0}^2 \rangle + \langle E_{y_0}^2 \rangle \tag{11a}$$
$$Q = \langle E_{x_0}^2 \rangle - \langle E_{y_0}^2 \rangle \tag{11b}$$
$$U = 2\langle E_{x_0} E_{y_0} \cos(\phi_x - \phi_y) \rangle \tag{11c}$$
$$V = 2\langle E_{x_0} E_{y_0} \sin(\phi_x - \phi_y) \rangle \tag{11d}$$

where $\langle \ldots \rangle$ denotes a time average. As usual, I represents the total intensity of radiation, Q and U represent the amount of linearly polarized radiation, and V represents the amount of circularly polarized radiation. For quasi-monochromatic light, each component of (11) is understood to be averaged over the entire frequency band. With respect to our calibration, we seek to evaluate I_x, I_y, Q, U, and V, where $I_x = \langle E_{x_0}^2 \rangle$ and $I_y = \langle E_{y_0}^2 \rangle$. From (11a), the Stokes parameter I is then simply given by $I = I_x + I_y$.

By looking at Fig. 1, we see that the $\hat{x}$-axis corresponds with TE-polarized electric fields, of which there are essentially three: the TE field from T_C transmitted through the sheet, the TE field from T_H reflected from the sheet, and the TE field emitted from the sheet itself. Similarly, the $\hat{y}$-axis corresponds with TM-polarized fields. Thus, we have

$$I_x = |t_{\mathrm{TE}}|^2 T_C + |r_{\mathrm{TE}}|^2 T_H + \epsilon_{\mathrm{TE}} T_S \tag{12}$$

where r_i is the ratio of the reflected to incident electric field polarized along $\hat{i}$ due to the sheet and likewise t_i is the ratio of transmitted to incident electric field polarized along $\hat{i}$. Using the

fact that $|r_i|^2 = R_i$ and $|t_i|^2 = 1 - R_i - \epsilon_i$ [the latter being due to (3)], we can recast (12) as

$$I_x = T_C + (T_H - T_C) R_{\mathrm{TE}} + (T_S - T_C) \epsilon_{\mathrm{TE}} \qquad (13)$$

which is the form given in (1). The derivation for I_y follows the same format and yields

$$I_y = T_C + (T_H - T_C) R_{\mathrm{TM}} + (T_S - T_C) \epsilon_{\mathrm{TM}}. \qquad (14)$$

Now we can use the fact that $Q = I_x - I_y$, which immediately leads to (1c). Next, due to the rotation properties of Q and U, we can write U as

$$U = I_{x_{45}} - I_{y_{45}} \qquad (15)$$

where $\hat{x}_{45}$ refers to the axis rotated $+45°$ from $\hat{x}$ and $\hat{y}_{45}$ is the orthogonal axis. However, as the $\hat{x}$ and $\hat{y}$ axes are exactly aligned with the TE and TM states, the $45°$-rotated axes will contain equal amounts of TE and TM fields and their intensity difference will be zero. Thus, we have

$$U = 0. \qquad (16)$$

Finally, we must consider the possibility of the sheet contributing a circular polarization signal V to our hypothetical polarimeter. We only expect this if there is some coherent phase delay between TE and TM polarizations to give the final polarization state some ellipticity. This cannot happen from the unpolarized loads, but the emission from the sheet, as seen at oblique angles, will, in general, be elliptically polarized due to its imperfect transparency [18]. However, this will be proportional to the emissivity of the sheet and, hence, will be small enough in comparison to the other Stokes parameters that it can be ignored for the purposes of this paper and we take

$$V \approx 0. \qquad (17)$$

APPENDIX II
DERIVATION OF SIMPLIFIED $R_{\mathrm{TE}} - R_{\mathrm{TM}}$

The purpose here is to derive the quantity $R_{\mathrm{TE}} - R_{\mathrm{TM}}$ under the simplifying assumptions that $\lambda \gg d$ (which is equivalent to $\delta \ll 1$) and $\theta = 45°$. Applying the latter assumption to (6) and (7) yields

$$\gamma_{\mathrm{TE}}^2 = n^2 - 0.5 \qquad (18a)$$

$$\gamma_{\mathrm{TM}}^2 = \frac{1}{n^4} \left(n^2 - 0.5 \right) \qquad (18b)$$

and

$$\delta = kd\sqrt{n^2 - 0.5}. \qquad (19)$$

Substituting these expressions into (5) and requiring that $\delta \ll 1$, we have

$$R_{\mathrm{TE}} \simeq (kd)^2 \frac{\left(n^2 - 1 \right)^2}{2} \qquad (20)$$

$$R_{\mathrm{TM}} \simeq (kd)^2 \frac{\left(n^2 - 1 \right)^4}{8n^4}. \qquad (21)$$

Finally, solving for $R_{\mathrm{TE}} - R_{\mathrm{TM}}$, we find

$$R_{\mathrm{TE}} - R_{\mathrm{TM}} \simeq (kd)^2 \frac{\left(n^2 - 1 \right)^2}{8n^4} \left[4n^4 - \left(n^2 - 1 \right)^2 \right] \qquad (22)$$

which factors into

$$R_{\mathrm{TE}} - R_{\mathrm{TM}} \simeq \left(\frac{\pi f d}{c} \right)^2 \frac{\left(n^4 - 1 \right) \left(n^2 - 1 \right) \left(3n^2 - 1 \right)}{2n^4} \qquad (23)$$

as desired.

REFERENCES

[1] P. M. Lubin and G. F. Smoot, "Polarization of the cosmic background radiation," *Astrophys. J.*, vol. 245, pp. 1–17, Apr. 1981.

[2] A. J. Gasiewski, "Calibration and applications of polarization-correlating radiometers," *IEEE. Trans. Microwave Theory Tech.*, vol. 41, pp. 767–773, May 1993.

[3] J. R. Wait, "Reflection from a wire grid parallel to a conducting plate," *Can. J. Phys.*, vol. 32, p. 571, 1954.

[4] T. Larsen, "A survey of the theory of wire grids," *IEEE. Trans. Microwave Theory Tech.*, vol. MTT-10, pp. 191–201, May 1962.

[5] J. Lesurf, *Millimeter-Wave Optics, Devices & Systems*. London, U.K.: IOP Publishing, 1990.

[6] M. Houde, R. L. Akeson, J. E. Carlstrom, J. W. Lamb, D. A. Schleuning, and D. P. Woody, "Polarizing grids, their assemblies and beams of radiation," *Pub. Astronom. Soc. Pacific*, vol. 113, pp. 622–638, 2001.

[7] M. M. Hedman, D. Barkats, J. O. Gundersen, S. T. Staggs, and B. Winstein, "A limit on the polarized anisotropy of the cosmic microwave background at subdegree angular scales," *Astrophys. J. Lett.*, vol. 548, pp. L111–L114, Feb. 2001.

[8] S. Cortiglioni, "Linear polarizaton and the effects of metal reflectors used to redirect the beam in microwave radiometers," *Rev. Sci. Instrum.*, vol. 65, no. 8, pp. 2667–2671, Aug. 1994.

[9] K. Rohlfs, *Tools of Radio Astronomy*. Berlin, Germany: Springer-Verlag, 1996.

[10] B. G. Keating, "A Search for the Large Angular Scale Polarization of the Cosmic Microwave Background," Ph.D. dissertation, Brown Univ., Providence, RI, 2000.

[11] R. M. A. Azzam and N. M. Bashara, *Ellipsometry and Polarized Light* Amsterdam, The Netherlands, 1977.

[12] M. Born and E. Wolf, *Principles of Optics*. New York: Pergamon, 1980.

[13] F. L. Pedrotti and L. S. Pedrotti, *Introduction to Optics*, 2nd ed. Englewood Cliffs, NJ: Prentice-Hall, 1993.

[14] P. F. Goldsmith, *Quasioptical Systems*. Piscataway, NJ: IEEE Press, 1998.

[15] A. Lehto, J. Tuovinen, and A. Räisänen, "Reflectivity of absorbers in 100–200 GHz range," *Electron. Lett.*, vol. 27, no. 19, pp. 1699–1700, Sept. 1991.

[16] F. I. Shimabukuro and C. Yeh, "Attenuation measurement of very low loss dielectric waveguides by the cavity resonator method applicable in the millimeter/submillimeter wavelength range," *IEEE. Trans. Microwave Theory Tech.*, vol. 36, pp. 1160–1166, July 1988.

[17] A. C. Lynch, "Measurement of permittivity by means of an open resonator—II: Experimental," in *Proc. R. Soc. Lond. A, Math. Phys. Sci.*, vol. 380, 1982, pp. 73–76.

[18] O. Sandus, "A review of emission polarization," *Appl. Opt.*, vol. 4, pp. 1634–1642, 1965.

[19] D. L. Jordan, G. D. Lewis, and E. Jakeman, "Emission polarization of roughened glass and aluminum surfaces," *Appl. Opt.*, vol. 35, pp. 3583–3590, July 1996.

[20] B. G. Keating, C. W. O'Dell, A. de Oliveira-Costa, S. Klawikowski, N. Stebor, L. Piccirillo, M. Tegmark, and P. T. Timbie, "A limit on the large angular scale polarization of the cosmic microwave background," *Astrophys. J. Lett.*, vol. 560, pp. L1–L4, Oct. 2001.

Christopher W. O'Dell was born in Binghamton, NY, in 1973. He received the B.S. degree in physics from the University of Dayton, Dayton, OH, in 1995, and the Ph.D. degree in physics from the University of Wisconsin–Madison, in 2001. His doctoral research involved building a microwave polarimeter for investigations of the large angular scale polarization properties of cosmic microwave background radiation.

He is currently a Post-Doctoral Researcher with the Department of Physics, University of Wisconsin–Madison. His research activities include instrumentation and data-analysis techniques related to cosmological research.

Daniel S. Swetz was born in Blenker, WI, in 1979. He received the B.S. degree in physics and astronomy from the University of Wisconsin–Madison, in 2002.

His research concerns the development of transition edge sensor bolometers for use in detecting the polarization of cosmic microwave background radiation.

Peter T. Timbie was born in Hartford, CT, in 1957. He received the B.A. degree in physics from Harvard University, Cambridge, MA.

From 1990 to 1996, he was an Assistant and Associate Professor with the Department of Physics, Brown University. From 1987 to 1990, he was a Post-Doctoral Fellow with the University of California at Berkeley, where he developed bolometers and cryogenics for experiments in space and scientific balloons. From 1985 to 1987, he was a Post-Doctoral Fellow, and from 1981 to 1985, he was a graduate student with Princeton University, where he developed a radio interferometer based on superconducting tunnel junction mixers to observe the cosmos. He is currently an Associate Professor with the Department of Physics, University of Wisconsin–Madison. His research concerns observational cosmology and focuses on measuring 2.7-K cosmic microwave background radiation using new types of sensitive microwave and millimeter-wave detectors.

Dr. Timbie is a member of the American Astronomical Society (AAS). He is a member of the IEEE Antennas and Propagation Society (IEEE AP-S). He was the recipient of the 1990 Presidential Young Investigator Award.